AMR Seminar #77

Case – 1

Contributed by: Cyril Fisher, M.D.

Clinical History: A male aged 69 presented with a submucosal lesion on the posterior pharyngeal wall. Previous biopsy suggested verrucous xanthoma. The lesion was excised.

Microscopic Features: This is a multinodular lesion in subcutis and skeletal muscle, composed of sheets of histiocyte-like cells with variable amounts of foamy cytoplasm including multinucleated cells and interspersed lymphocytes. Eosinophils are not prominent. There are interspersed spindle cells with very occasional mitoses, but no significant nuclear atypia is seen, and no necrosis is evident.

Histological and Immunohistochemical Findings: Immunohistochemistry is diffusely positive for desmin (including in many foamy cells), MyoD1 (nuclear), SMA, CD68 and ALK. Negative are myogenin, h-caldesmon, SMM, CK, S100 protein, ERG, HMB45, melan-A, CD34, CD3, CD20, CD30, CG, CD56, and CD117. EBER ISH is negative.

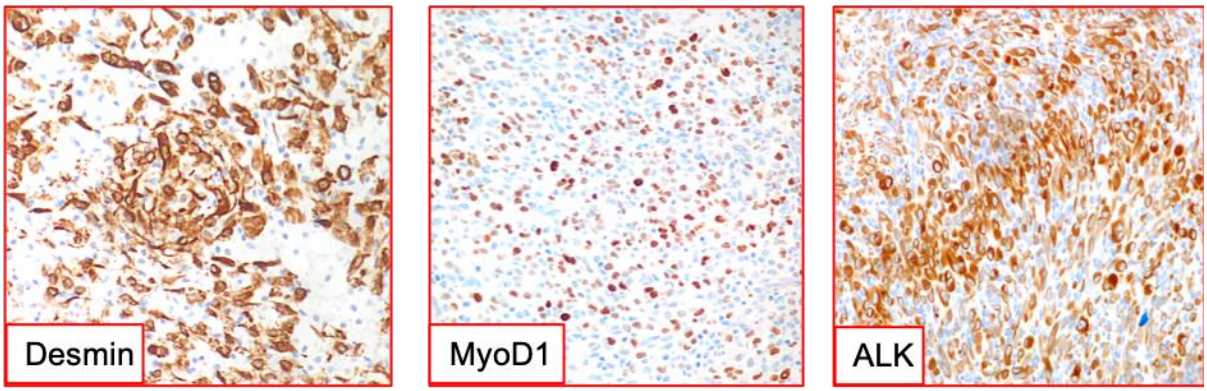

FISH shows *ALK* gene rearrangement with partner gene unknown. It is negative for *EWSR1* and *FUS* gene rearrangement. RT-PCR shows no *FOXO1-PAX3* or -*PAX7* transcripts.

Diagnosis: Histiocyte-rich rhabdomyoblastic tumor (inflammatory leiomyosarcoma) with ALK gene rearrangement.

Comments: The morphology and myoid immunophenotype appear to correspond to the tumor recently described as histiocyte-rich rhabdomyoblastic tumor. Nine of the ten cases were males. Patients were aged 23-69 years, and tumors arose in deep soft tissue of trunk, lower limbs and neck. This was designated as a lesion of uncertain malignant potential though none of the reported cases recurred or metastasized.[1,2]

Similar tumors have been described as inflammatory leiomyosarcoma. In a small number of published reports, e.g.[3,4,5], initially thought to be a variant of inflammatory malignant fibrous histiocytoma[3], this has a different phenotype from usual smooth muscle tumors, sometimes lacking SMA, MSA and h-caldesmon, and additionally can demonstrate primitive skeletal muscle differentiation with variable MyoD1 and myogenin expression. Inflammatory cells and desmin-positive foamy cells are regular features. 'Leiomyosarcoma' might be a misnomer if there is rhabdomyoblastic differentiation and the term low-grade inflammatory myogenic tumor has recently been proposed.[5]

Inflammatory leiomyosarcoma has been noted to have a near-haploid phenotype and a primitive myogenic gene signature.[6] However, ALK positivity is unexpected and has not been found in such cases[5]. The *ALK* gene rearrangement raises the differential diagnosis of inflammatory myofibroblastic tumor, but the morphology differs and diffuse desmin expression and MyoD1 positivity are not features of IMT. *ALK* overexpression

without underlying *ALK* rearrangement has been described in a rare variant of rhabdomyosarcoma which differs in having epithelioid morphology, high mitotic index and a defining *FUS* (or *EWSR1*)-*TFCP2* fusion.[7]

The differential diagnosis also includes the rare ALK-positive histiocytosis with *KIF5B-ALK* (rarely *COL1A2-ALK*) fusion[8] which occurs mostly in infants and occasionally in young adults. This can manifest spindle cell morphology and SMA positivity but has more Touton giant cells, less prominent foamy histiocytes, sometimes has focal S100 protein positivity, and lacks desmin in the cases tested.[9,10]

The desmin/ALK immunophenotype can also be found in angiomatoid fibrous histiocytoma, but this differs morphologically, lacks skeletal muscle differentiation, and has *EWSR1* gene rearrangement without *ALK* gene rearrangement.

References:

1. Martinez AP, Fritchie KJ, Weiss SW, et al. Histiocyte-rich rhabdomyoblastic tumor: rhabdomyosarcoma, rhabdomyoma, or rhabdomyoblastic tumor of uncertain malignant potential? A histologically distinctive rhabdomyoblastic tumor in search of a place in the classification of skeletal muscle neoplasms. *Mod Pathol*. 2019;32(3):446-457.

2. Bourgeau M, Martinez AP. Histiocyte-rich rhabdomyoblastic tumor: a report of two cases and a review of the differential diagnoses [published online ahead of print, 2020 Jun 9] [published correction appears in Virchows Arch. 2020 Jun 22]. *Virchows Arch*. 2020;10.1007/s00428-020-02857-x.

3. Merchant W, Calonje E, Fletcher CD. Inflammatory leiomyosarcoma: a morphological subgroup within the heterogeneous family of so-called inflammatory malignant fibrous histiocytoma. *Histopathology*. 1995;27(6):525-532.

4. Chang A, Schuetze SM, Conrad EU 3rd, Swisshelm KL, Norwood TH, Rubin BP. So-called "inflammatory leiomyosarcoma": a series of 3 cases providing additional insights into a rare entity. *Int J Surg Pathol*. 2005;13(2):185-195.

5. Michal M, Rubin BP, Kazakov DV, et al. Inflammatory leiomyosarcoma shows frequent co-expression of smooth and skeletal muscle markers supporting a primitive myogenic phenotype: a report of 9 cases with a proposal for reclassification as low-grade inflammatory myogenic tumor. *Virchows Arch*. 2020;477(2):219-230.

6. Arbajian E, Köster J, Vult von Steyern F, Mertens F. Inflammatory leiomyosarcoma is a distinct tumor characterized by near-haploidization, few somatic mutations, and a primitive myogenic gene expression signature. *Mod Pathol*. 2018;31(1):93-100.

7. Le Loarer F, Cleven AHG, Bouvier C, et al. A subset of epithelioid and spindle cell rhabdomyosarcomas is associated with *TFCP2* fusions and common ALK upregulation. *Mod Pathol*. 2020;33(3):404-419.

8. Chang KTE, Tay AZE, Kuick CH, et al. ALK-positive histiocytosis: an expanded clinicopathologic spectrum and frequent presence of *KIF5B-ALK* fusion. *Mod Pathol*. 2019;32(5):598-608.

9. Gupta GK, Xi L, Pack SD, et al. ALK-positive histiocytosis with *KIF5B-ALK* fusion in an adult female. *Haematologica*. 2019;104(11):e534-e536.

10. Kashima J, Yoshida M, Jimbo K et al. ALK-positive histiocytosis of the breast. A clinicopathologic study highlighting spindle cell histology. *Am J Surg Pathol* 2020 (published online ahead of print)

AMR Seminar #77

Case – 2

Contributed by: Ondřej Hes, M.D.

Clinical History: 24-year-old female was referred to hospital for right flank pain. CT showed huge mass in right retroperitoneum involving suprarenal gland, hilus of the kidney. Size according examination CT was 56 x 78 x 72 mm. Adrenal gland carcinoma was established as working diagnosis.

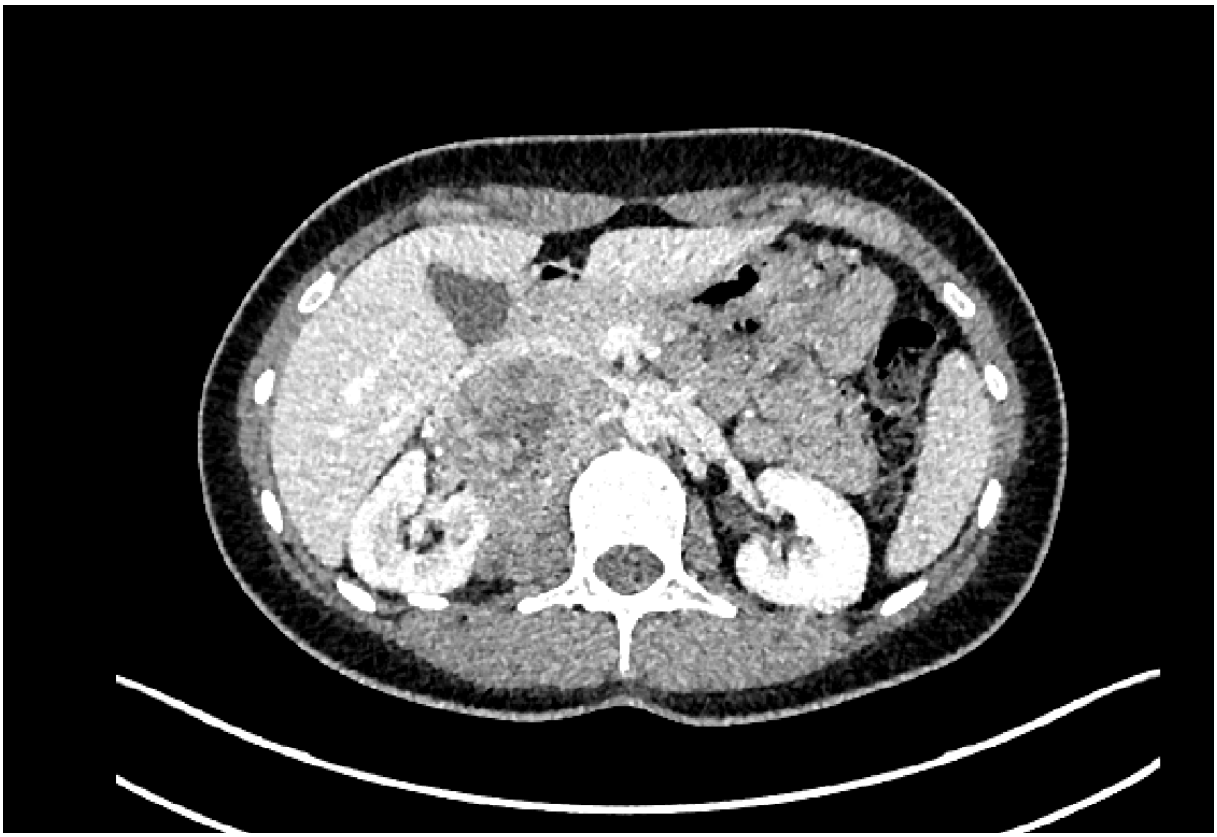

Resection of retroperitoneal mass, right suprarenal gland and right kidney was performed.

Gross Description: Specimen measured 15 x 13 x 7 cm, formed by kidney, tumor, suprarenal gland and fatty tissue. Tumorous mass was friable, whitish with focal hemorrhagia, size 85 x 65 x 55 mm infiltrating fatty tissue, adrenal gland and hilus of the kidney. Vast majority of tumorous mass was extrarenal.

Histological and Immunohistochemical Findings: Tumor is variable in architecture. Mostly alveolar, in some areas tubular and papillary. Tumor grows to renal sinus in the one end, in the other end involved suprarenal gland. Interesting area is captured on slide I´ve sent to you……there is infiltration of autonomic nerves, ganglia and in some aspect tumor resembles ganglioneuroma or similar lesion. Tumor is composed of eosinophilic cells with prominent nuclei and deep red macronucleoli with perinucleolar clearing. Focally, cells with voluminous finely granular cytoplasm were encountered (rhabdoid appearance).

Tumor was positive for PAX 8, EMA, CD10, and CD34. Negative reaction was for Melan A, HMB45, synaptophysin, chromogranin, INSM1, S-100, inhibin, CK20, GATA 3, vimentin, OSCAR, and AE1-AE3. TFE3 was focally positive, however reaction was far from perfect. FH and SDHB were nicely retained.

TFE3 gene. FISH showed break, however amplification was not present. Partner was not examined.

TFEB gene was intact, no amplification was confirmed.

Diagnosis: Translocation TFE3 (Xp11) renal cell carcinoma (RCC)

Comments: RCC with *TFE3* rearrangements (Xp11.2) is the most common of all MitF RCCs. Although morphologic features of translocation TFE3 translocation RCCs was considered relative characteristic and compact at the beginning, later studies described morphologic variants associated with different fusion partners. Numerous partners were described, like *ASPSCR1*, *PRCC*, *NONO*, *SFPQ*, *CLTC*, *PARP14*, *LUC7L3*, *KHSRP*, *DVL2*, *MED15*, *NEAT1*, *RBM10*, *KAT6A*, and *GRIPAP1* (77-85). Some TFE3 translocation carcinoma resembles clear cell papillary RCC or even urothelial carcinoma (NONO-TFE3). In some cases, morphology resembling just slightly unusual CCRCC can be seen.

Nowadays it is apparent, that TFE3 translocation RCCs can show a highly heterogeneous morphologic spectrum. Renal cell carcinomas occurring in kids or young adults must be always considered, as potential tumor from translocation family. RCCs with solid-papillary architecture, clear cells and eosinophilic cells, numerous psammoma bodies also should be considered as suspect.

However, some cases are highly unusual and with broad scale testing, surprises (morphology vs status of *TFE3* gene) can't be ruled out. Immunohistochemical reaction with TFE3 may not be sufficient to confirm/exclude the diagnosis, because antibody is not very robust and false negative and even false positive cases are not rare. Also, FISH results should be interpreted with caution. In case that fusion partner is too close or too far (beyond reaches of probe), results can be false negative (namely partners *RBM10, RBMX, GRIPAP1,* and *NONO*). We use (in highly suspect cases and negative FISH) NGS Archer, which seems to be much more sensitive.

This case was particularly difficult. It was diagnosed as suprarenal tumor and surgery was focused on suprarenal tumor. During grossing, it was not possible to find primary location of the tumor. Majority of tumorous mass was located in soft tissues between kidney and adrenal gland, both organs were infiltrated by carcinoma.

Very confusing was the block with structures of ganglia, overgrowed by renal cell carcinoma.

Differential diagnosis in this particular case was broad.

1. Adrenal gland carcinoma. Our tumor was too complex with tubulopapillary pattern. Cells with eosinophilic cytoplasm mixed with eosinophilic cells would be not typical for adrenal carcinoma.

Immunohistochemical profile pointed to RCC.

2. Urothelial carcinoma. This was my favorite differential diagnosis at the beginning. However renal pelvis did not show any dysplasia, urothelial carcinoma in situ, etc. Also, immunohistochemical profile was not consistent with urothelial carcinoma.

3. Other subtype of RCC. With complex immunohistochemical profile and genetic testing, diagnosis was straightforward. Theoretically, if genetic analysis failed to confirm *TFE3* translocation, unclassified RCC would be most likely final diagnosis.

References:

1. Argani P, Antonescu CR, Illei PB, Lui MY, Timmons CF, Newbury R, et al. Primary renal neoplasms with the ASPL-TFE3 gene fusion of alveolar soft part sarcoma: a distinctive tumor entity previously included among renal cell carcinomas of children and adolescents. Am J Pathol. 2001;159(1):179-92.
2. Argani P, Lui MY, Couturier J, Bouvier R, Fournet JC, Ladanyi M**.** A novel CLTC-TFE3 gene fusion in pediatric renal adenocarcinoma with t(X;17)(p11.2;q23). Oncogene. 2003;22(34):5374-8.
3. Argani P, Ladanyi M**.** Renal carcinomas associated with Xp11.2 translocations / *TFE3* gene fusions. In: Eble JN, Sauter G, Epstein JI, Sesterhenn IA, eds. Pathology and Genetics of Tumours of the Urinary System and Male Genital Organs. 1st ed. Lyon: IARC Press; 2004:37-8.
4. Argani P, Olgac S, Tickoo SK, Goldfischer M, Moch H, Chan DY, et al. Xp11 translocation renal cell carcinoma in adults: expanded clinical, pathologic, and genetic spectrum. Am J Surg Pathol. 2007;31(8):1149-60.

5. Argani P, Hicks J, De Marzo AM, Albadine R, Illei PB, Ladanyi M, et al. Xp11 translocation renal cell carcinoma (RCC): extended immunohistochemical profile emphasizing novel RCC markers. Am J Surg Pathol. 2010;34(9):1295-303.
6. Ellis CL, Eble JN, Subhawong AP, Martignoni G, Zhong M, Ladanyi M, et al. Clinical heterogeneity of Xp11 translocation renal cell carcinoma: impact of fusion subtype, age, and stage. Mod Pathol. 2014;27(6):875-86.
7. Argani P**.** MiT family translocation renal cell carcinoma. Semin Diagn Pathol. 2015;32(2):103-13.
8. Argani P, Zhong M, Reuter VE, Fallon JT, Epstein JI, Netto GJ, et al. TFE3-Fusion Variant Analysis Defines Specific Clinicopathologic Associations Among Xp11 Translocation Cancers. Am J Surg Pathol. 2016;40(6):723-37.
9. Hayes M, Peckova K, Martinek P, Hora M, Kalusova K, Straka L, et al. Molecular-genetic analysis is essential for accurate classification of renal carcinoma resembling Xp11.2 translocation carcinoma. Virchows Arch. 2015;466(3):313-22.
10. Kato I, Furuya M, Baba M, Kameda Y, Yasuda M, Nishimoto K, et al. RBM10-TFE3 renal cell carcinoma characterised by paracentric inversion with consistent closely split signals in break-apart fluorescence in-situ hybridisation: study of 10 cases and a literature review. Histopathology. 2019;75(2):254-65.

AMR Seminar #77

Case – 3

Contributed by: Jesse McKenney, M.D.

Clinical History: 62-year-old-man with 12.9 cm renal mass discovered during work-up for flank pain.

Diagnosis: Renal cell carcinoma, MiT family translocation type (TFEB re-arrangement identified by FISH).

Comments: I shared this case because the morphologic appearance is not what is classically described in renal cell carcinomas (RCCs) with a TFEB translocation. In the current WHO classification, RCC with either TFE3 or TEFB re-arrangements are classified as "MiT family translocation RCC" given their histologic and immunophenotypic similarities and their alterations in a related genetic pathway. These tumors were originally described in children (making up a higher percentage of RCCs in that group), but it is now recognized they are seen more frequently in adults. While t(6;11) RCC (i.e. TFEB RCC) was originally described as having a distinctive biphasic architecture [characterized by grade 3 cells surrounding an aggregate of smaller lower grade cells associated with basement membrane-like material], the evolving experience suggests a much broader morphologic spectrum. In a recent study assessing fusion partners, MALAT1-TFEB fusion cases had variable morphology, but all of the classic biphasic tumors were in that group (Xia et al.). Other fusion partners (ACTB-TFEB, EWSR1-TFEB, CLTC-TFEB, and PPP1R10-TFEB) had a more varied morphologic appearance with no classic biphasic patterns. Even more recently, RCCs with TFEB amplification have been reported, which have a different morphology (characterized by nests of high-grade eosinophilic cells forming variable papillae with associated necrosis) and an aggressive clinical behavior.

References:

1. Argani P, Hawkins A, Griffin CA, et al. A distinctive pediatric renal neoplasm characterized by epithelioid morphology, basement membrane production, focal HMB45 immunoreactivity, and t(6;11)(p21.1;q12) chromosome translocation. *Am J Pathol*. 2001;158(6):2089-2096.
2. Argani P, Yonescu R, Morsberger L, et al. Molecular confirmation of t(6;11)(p21;q12) renal cell carcinoma in archival paraffin-embedded material using a break-apart TFEB FISH assay expands its clinicopathologic spectrum. *Am J Surg Pathol*. 2012;36(10):1516-1526.
3. Rao Q, Liu B, Cheng L, et al. Renal cell carcinomas with t(6;11)(p21;q12): A clinicopathologic study emphasizing unusual morphology, novel alpha-TFEB gene fusion point, immunobiomarkers, and ultrastructural features, as well as detection of the gene fusion by fluorescence in situ hybridization. *Am J Surg Pathol*. 2012;36(9):1327-1338.
4. Xia et al. Clinicopathologic and molecular analysis of the TFEB fusion variant reveals new members of the TFEB translocation renal cell carcinomas: expanding the genomic spectrum. *Am J Surg Pathol* 2020;444(4):477-489.
5. Williamson SR, Grignon DJ, Cheng L, et al. Renal cell carcinoma with chromosome 6p amplification including the TFEB gene: a novel mechanism of tumor pathogenesis? *Am J Surg Pathol*. 2017;41(3):287-298.
6. Skala SL, Xiao H, Udager AM, et al. Detection of 6 TFEB-amplified renal cell carcinomas and 25 renal cell carcinomas with MITF translocations: systematic morphologic analysis of 85 cases evaluated by clinical TFE3 and TFEB FISH assays. *Mod Pathol*. 2018;31(1):179-197.

Review article:

1. Gandhi JS, Malik F, Amin MB, Argani P, Bahrami A. MiT family translocation renal cell carcinomas: A 15th anniversary update. *Histol Histopathol*. 2020;35(2):125-136.

AMR Seminar #77

Case – 4

Contributed by: Michael Michal, M.D., PhD.

Clinical History: A 40-year-old man with a soft tissue tumor involving and unspecified skeletal muscle, size unknown.

Histological and Immunohistochemical Findings: Microscopy showed a well-circumscribed and encapsulated (not shown) predominantly spindle cell neoplasm with a mostly haphazard growth pattern and only focal storiform or fascicular areas. The nuclei were spindled to ovoid with only a mild nuclear pleomorphism. Mitotic index was very low (less than 1/10 HPF). Most cells had a palely eosinophilic cytoplasm but, in some areas, minor population of cells with a slightly darker and more abundant cytoplasm had a rhabdoid or "strap cell" appearance (lacking cross-striations). Admixed among these cells was an abundant lymphoplasmacytic infiltrate. In some areas, large histiocytic aggregates were present, some of them combined with cholesterol deposits and calcifications.

Immunohistochemically, the tumor cells were diffusely positive for desmin, muscle specific actin, pax-7 and myoD1 and focally positive with myogenin. Proliferative index was less than 2%. Other markers (AE1/3, S100 protein, SMA, MDM2, CD21, CD35, CD34, ALK-1 were completely negative.

Diagnosis: Inflammatory leiomyosarcoma (according to the current WHO)/Inflammatory rhabdomyoblastic tumor (most likely name in the next WHO).

Comments: Although described already in 1995, this fascinating entity has remained half-forgotten for almost a quarter of century until very recently. Since then, it has undergone several major developments. Here is their summary:

In 1995, Merchant et al. published a series of 12 tumors with morphological and immunohistochemical features reminiscent of smooth muscle differentiation admixed with a prominent inflammatory component that had previously fallen within the category of inflammatory malignant fibrous histiocytoma. Based on the cytomorphological features coupled with the immunohistochemical expression of desmin, muscle-specific actin and smooth muscle actin by some of the neoplastic cells, these tumors were thought to represent smooth muscle neoplasms and the term Inflammatory leiomyosarcoma was coined [1]. A few years later, the first cytogenetic analysis of ILMS was performed and revealed a highly unusual and characteristic chromosomal pattern consisting of a near haploid genome [2]. Importantly, this and further studies have also shown a clearly nonrandom retention of both parental copies of chromosomes 5 and 22 which are present in almost all cases (and 18, 20-21 in a subset of cases), while all other autosomes feature a loss of heterozygosity [2–5]. Arbajian et al. recently published a thorough molecular analysis of these tumors which has incited the current developments. Besides other methods, this group performed gene expression profiling which showed a high expression of genes such as *MYOD1*, *MYOG*, *PAX-7*, *MYF5* or *MYF6*, all of which are known to be crucial for skeletal muscle development. Surprisingly, however, they did not test the expression of respective proteins encoded by these genes on the immunohistochemical level [4]. Since our group had been interested in these neoplasms for some time, this has prompted us to publish a clinicopathological paper focused mainly on immunohistochemical features and a long-term follow-up. In this study, we have shown for the first time that these tumors express not only desmin and (some of them) smooth muscle actin but also skeletal muscle markers myoD1, myogenin and pax-7 and so that they in fact do not represent leiomyosarcomas. We have also confirmed the excellent long-term outcome of most of these tumors (some of our cases had follow-up longer than 20 years) [6].

Shortly before our paper, the group of Dr. Folpe reported a study in which they presented an allegedly novel group of tumors which they coined Histiocyte-rich rhabdomyoblastic tumors [7]. However, as we have noted in our paper, these tumors showed virtually identical clinicopathological features as ILMS and this was later

confirmed in a follow-up study by the Folpe group [5]. In this report, they have taken cases of their so called Histiocyte-rich rhabdomyoblastic tumor and performed a karyotype analysis which showed the same near-haploid genome with nonrandom retention of both copies of the particular chromosomes. Besides confirming that all these reports in fact describe the same entity, they also proposed a new name for it, which will likely be accepted in the next WHO: Inflammatory rhabdomyoblastic tumor.

As a result of these recent discoveries, the characteristic features of these tumors become much better defined and can be summarized as follows:

- Clinically there is a distinct predilection for deep soft tissues, particularly of the thigh or back of younger male patients (median 35-40 years). However, well-characterized examples have been also described in the pelvis, lungs or neck so the anatomical distribution seems to be broad.
- Morphologically, the presented case may serve as the prototypical example. Some cases may also show abundant giant cells.
- Immunohistochemically, the great majority of cases stains with desmin and at least one of the more specific skeletal muscle markers (myoD1, myogenin, pax-7). SMA can be positive is some cases. CD163 and other histiocytic markers decorate the abundantly present histiocytes. Cytokeratins, S100 protein and other frequently used markers are typically negative.
- Molecular genetics – several cases were shown to harbor NF1 gene mutation. No recurrent gene fusions were reported. The above described karyotype seems to be very specific for this entity. However, karyotype analysis is technically challenging and not widely available.
- Although it should be considered intermediate grade malignancy, the vast majority of cases will neither recur nor metastasize (as the presented case with a 22 years of uneventful follow-up). However, exceptional cases may metastasize/spread locally and only few weeks ago, the Folpe group published a typical example of this tumor showing transition to a clear-cut pleomorphic rhabdomyosarcoma [5]. Therefore, it seems, that the fascinating evolution of this entity is not yet completely finished!

References:

1) Inflammatory leiomyosarcoma: a morphological subgroup within the heterogeneous family of so-called inflammatory malignant fibrous histiocytoma. Merchant W, Calonje E, Fletcher CD. Histopathology. 1995 Dec;27(6):525-32.
2) Inflammatory leiomyosarcoma may be characterized by specific near-haploid chromosome changes. Dal Cin P, Sciot R, Fletcher CD, Samson I, et al. Pathol. 1998 May;185(1):112-5. Review.
3) So-called "inflammatory leiomyosarcoma": a series of 3 cases providing additional insights into a rare entity. Chang A, Schuetze SM, Conrad EU 3rd, et al. Int J Surg Pathol. 2005 Apr;13(2):185-95.
4) Inflammatory leiomyosarcoma is a distinct tumor characterized by near-haploidization, few somatic mutations, and a primitive myogenic gene expression signature. Arbajian E, Köster J, Vult von Steyern F, Mertens F. Mod Pathol. 2018 Jan;31(1):93-100. doi: 10.1038/modpathol.2017.113. Epub 2017 Sep 8.
5) "Inflammatory Leiomyosarcoma" and "Histiocyte-rich Rhabdomyoblastic Tumor": a clinicopathological, immunohistochemical and genetic study of 13 cases, with a proposal for reclassification as "Inflammatory Rhabdomyoblastic Tumor". Cloutier JM, Charville GW, Mertens F, Sukov W, Fritchie K, Perry KD, Edgar M, Rowsey RA, Folpe AL. Mod Pathol. 2021 Apr;34(4):758-769. doi: 10.1038/s41379-020-00703-8. Epub 2020 Oct 22. PMID: 33318583.
6) Inflammatory leiomyosarcoma shows frequent co-expression of smooth and skeletal muscle markers supporting a primitive myogenic phenotype: a report of 9 cases with a proposal for reclassification as low-grade inflammatory myogenic tumor. Michal M, Rubin BP, Kazakov DV, Michalová K, Šteiner P, Grossmann P, Hájková V, Martínek P, Švajdler M, Agaimy A, Hadravský L, Kalmykova AV, Konishi E, Heidenreich F, Michal M. Virchows Arch. 2020 Aug;477(2):219-230. doi: 10.1007/s00428-020-02774-z. Epub 2020 Feb 20. PMID: 32078043.
7) Histiocyte-rich rhabdomyoblastic tumor: rhabdomyosarcoma, rhabdomyoma, or rhabdomyoblastic tumor of uncertain malignant potential? A histologically distinctive rhabdomyoblastic tumor in search of a place in the classification of skeletal muscle neoplasms. Martinez AP, Fritchie KJ, Weiss SW, Agaimy A, Haller F, Huang HY, Lee S, Bahrami A, Folpe AL. Mod Pathol. 2019 Mar;32(3):446-457. doi: 10.1038/s41379-018-0145-0. Epub 2018 Oct 4. PMID: 30287926.
8) Inflammatory rhabdomyoblastic tumor with progression to high-grade rhabdomyosarcoma. Geiersbach K, Kleven DT, Blankenship HT, Fritchie K, Folpe AL. Mod Pathol. 2021 Mar 23. doi: 10.1038/s41379-021-00791-0. Epub ahead of print. PMID: 33758326.

AMR Seminar #77

Case – 5

Contributed by: Markku Miettinen, M.D.

Clinical History: 79-year-old male with a history of vocal card squamous cell carcinoma developed a large mass in the right pleural cavity. There was no lung involvement. The mass was initially biopsied and liposarcoma was suspected. Subsequently the mass was removed/debulked yielding solid grayish and mucinous tissue including a fragment measuring 25 x 15 x 6.5 cm and yellow gray to tan gelatinous fragments measuring in aggregate 15 x 10 x 3 cm. The mass was externally attached to lung but not believed to originate from it. Pleural involvement was noted with the mass involving tissues lined by reactive and fibrinous mesothelial surfaces. A concurrent biopsy confirmed recurrent/residual moderately differentiated vocal cord squamous carcinoma.

Histological and Immunohistochemical Findings: The sampling revealed mainly sarcomatoid spindle cell proliferation with areas of necrosis. This was largely unorganized, with smaller foci of fascicular architecture. There were also epithelioid nests, some of which had clearly squamous cell differentiation while others were less differentiated with occasional pseudoglandular appearance.

The spindle cell components were weakly to moderately keratin AE1/AE3 positive and the epithelioid clusters were strongly positive. The epithelioid cells were also positive for CK5/6 and p63, while negative for calretinin and nuclear WT1. Only reactive mesothelia were positive for the latter 2 markers. Additional immunostains for MDM2, S100 protein, and SOX10 were negative.

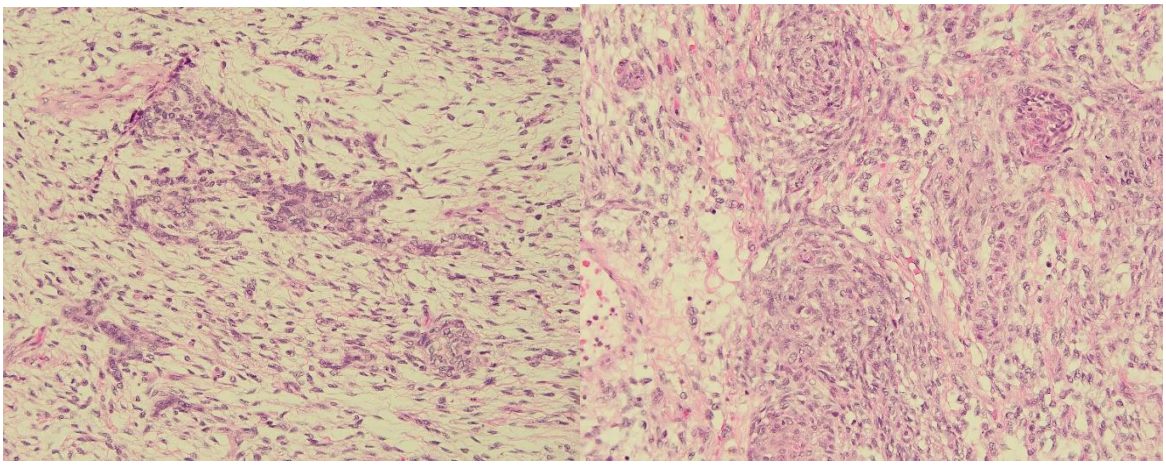

Diagnosis: Sarcomatoid squamous cell carcinoma in pleural cavity, primary vs. metastatic

Comments: The differentiated component of this tumor is squamous cell carcinoma, and the best assumption is that the rest of tumor is sarcomatoid squamous cell carcinoma. There is no evidence of mesothelioma or mixed tumor/myoepithelioma. After molecular studies, it cannot still be sure if this is a metastatic sarcomatoid squamous carcinoma (initially favored interpretation) or possibly a primary pleural/lung surface sarcomatoid squamous carcinoma. There is one common mutation variant between the pleural and vocal cord tumors in gene XPO1, an obscure gene I never heard before. The pleural cavity tumor had a BAP1 mutation with a low VAF. This mutation is not known in malignant mesothelioma. Thoracic pathology experts and others please weigh in with your experience.

Genomic Studies: True Sight Oncology 500 sequencing panel was performed for both pleural cavity mass and the vocal cord squamous cell carcinoma. The pleural sarcomatoid squamous cell carcinoma had 3 significant variants: BAP1 R237C (5% VAF), PTCH1 G115* (50% VAF), and XPO1 D571V (3.5% VAF). The laryngeal squamous cell carcinoma had 6 variants: CDKN2A pG69* (35% VAF), PIK3CA T108H (24% VAF), PRKDC splice site variant (14% VAF), TP53 V157F (39% VAF), SMAD4 Q516fs (14% VAF), and XPO1 D571V (8% VAF). VAF = variant allelic frequency.

AMR Seminar #77

Case – 6

Contributed by: Vania Nosé, M.D.

Clinical History: This 51-year-old patient with past history of bilateral glomus jugulare, with resection of a tumor at the left skull base in 1991, as 28-year-old patient, followed by a similar resection on the right side of 1994, he presented with a sense of heart palpitation and discomfort in the chest and underwent a full ER evaluation. This included a neck and chest CT with noted large mass in the lower neck extending into the mediastinum. He was submitted to an extensive surgery in 2016 for resection of the numerous paragangliomas including head and neck, left carotid sheath paraganglioma with the lower neck and marked intrathoracic component, additional paraganglioma of the periaortic region paragangliomas.

AMR Seminar #77

Case – 7

Contributed by: Kyle Perry, M.D.

Short Summary: 20-year-old found to have proximal femur lesion after fall.

Clinical History and Radiology: The patient is a 20-year-old who experienced a fall. During assessment, CT imaging demonstrated a well-delineated intraosseous lesion with mixed areas of sclerosis and lucency (Figure 1A and 1B). The surrounding soft tissue demonstrated edematous changes, suggestive of fracture. Some endosteal scalloping was present.

In order to further assess this lesion, a needle biopsy was performed. This predominantly showed fragments of cartilage with mildly increased cellularity but otherwise relatively bland appearing nuclei (Figure 2A). There were, however, areas of "fibrous tissue" that appeared benign but not entirely typical of the usual fibroblastic changes seen in a fracture callus (Figure 2B). Given the suggestion of likely microfracture by imaging, I reported the findings to the clinician as favoring low-grade cartilaginous neoplasm. The subsequent curettage, however, showed similar appearing irregular fragments of cartilage without substantial associated cytologic atypia (Figure 3A and 3B). Surrounding this cartilage were areas of fibromyxoid and fibrous stroma with trabecular islands of woven bone (Figures 3C and 3D).

Diagnosis: Fibrous dysplasia with areas of cartilaginous differentiation.

Comments: While fibrous dysplasia can have focal cartilaginous nodules, these tumors can occasionally have a cartilaginous component which is a more prominent (if not a predominant) portion of the overall tumor. These tumors have been referred to as fibrocartilaginous dysplasia or fibrous dysplasia with massive cartilaginous differentiation. Personally, I'm not sure if the curettage specimen would meet the criteria for "massive." However, it was sufficient for us to primarily consider a low-grade cartilaginous tumor on a limited needle core biopsy.

Fibrocartilaginous dysplasia generally occurs in adolescents and younger adults and most frequently arises in the femur or tibia. Radiologic imaging typically reveals the ground glass appearance usually associated with conventional fibrous dysplasia. Often, cases of fibrocartilaginous dysplasia will also exhibit a ring-like calcification pattern consistent with a prominent cartilaginous element.

Microscopically, fibrocartilaginous dysplasia consists of large and irregular portions of chondroid tissue in the background of otherwise classic features of fibrous dysplasia. Similar to this case, the cartilage shows irregular margins with increased cellularity and can contain mild atypia. Areas of enchondral ossification (seen on the initial biopsy) can also be seen.

The primary importance of recognizing fibrocartilaginous dysplasia rests in not confusing this entity for a more aggressive cartilaginous neoplasm. As fibrous dysplasia often exhibits an endosteal scalloping that could be interpreted as potentially aggressive for a chondroid lesion, an awareness of this phenomenon can prevent an excessively aggressive resection by the surgeon. Of note, one case of fibrocartilaginous dysplasia was submitted in seminar #20 by Dr. Weidner which may have had a more impressive cartilaginous component. Given the increased usage of image guided needle core biopsies for diagnosis of bone lesions, I thought a second case could be of interest (1-3).

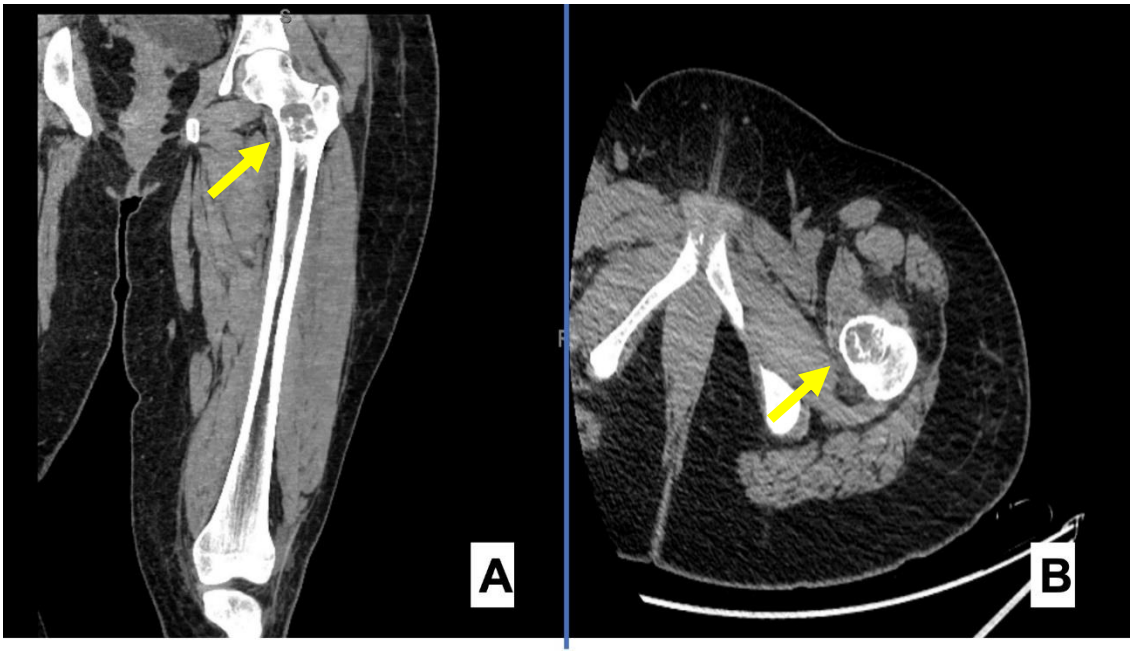

Figure 1: CT scan showing mixed lytic and sclerotic lesion (yellow arrow) in the proximal femur with endosteal scalloping, possible fracture and associated soft tissue edema (A). The axial view further highlights endosteal scalloping (yellow arrow) (B).

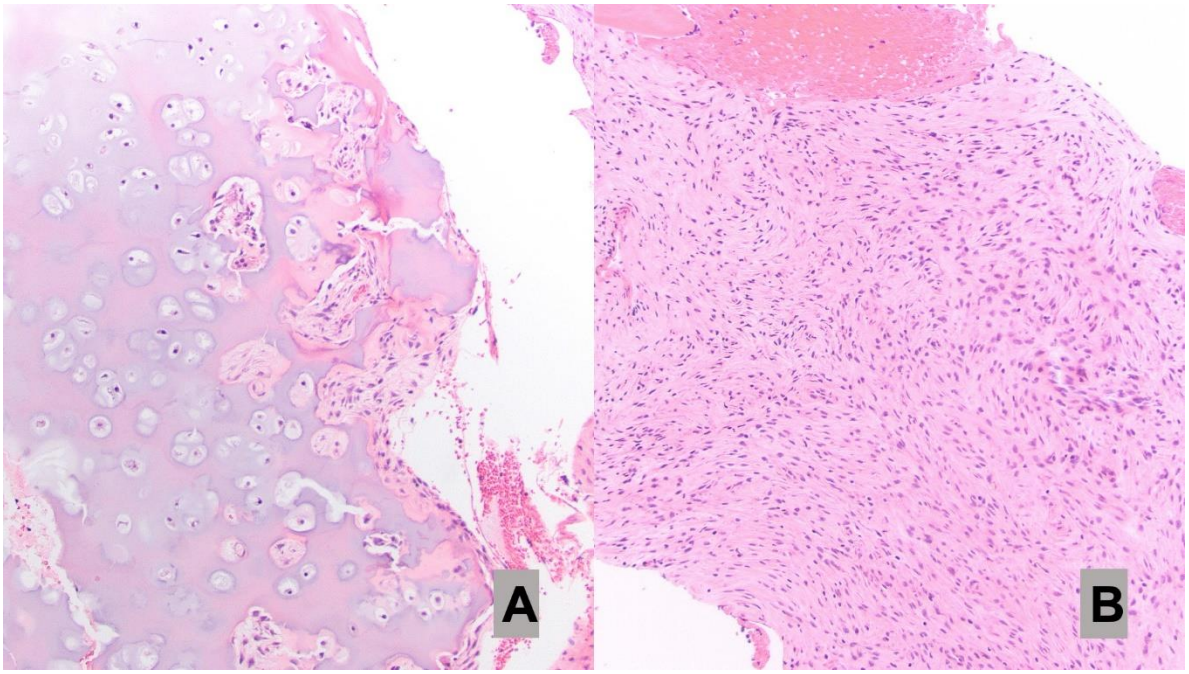

Figure 2: Needle core biopsy showing prominent cartilage with mild increase in cellularity (A). Adjacent to this cartilage are focal areas of fibrous like tissue (B).

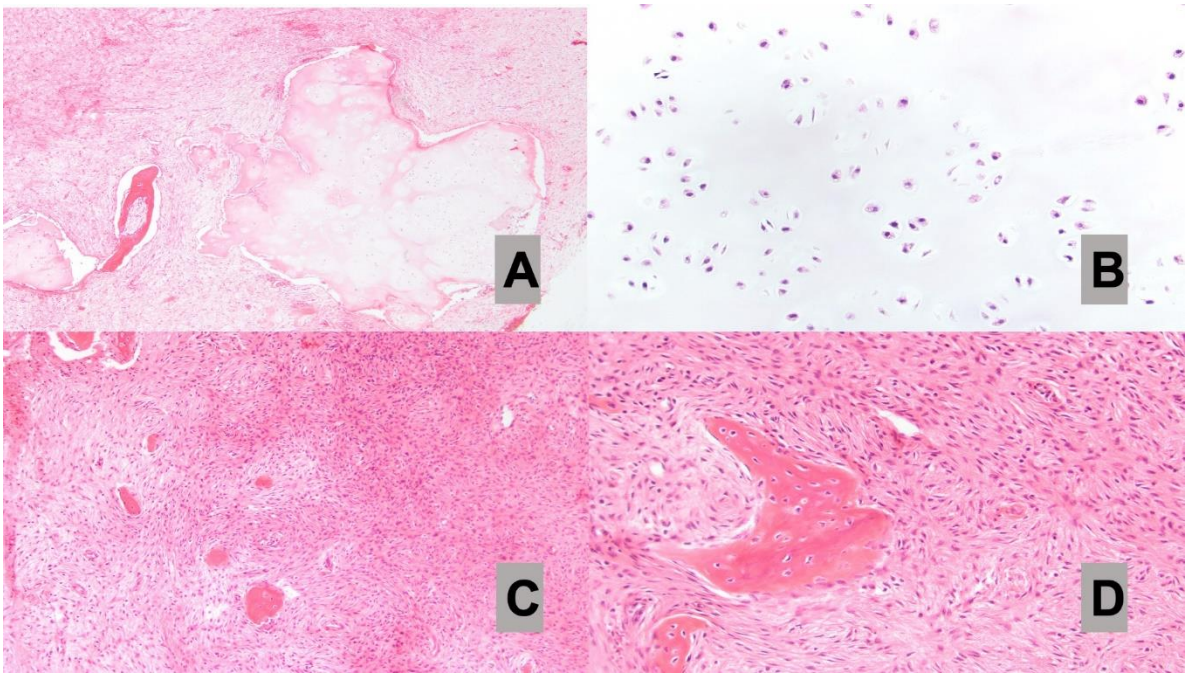

Figure 3: Prominent fragments of cartilage were found in the curettage specimen (A). Closer examination shows increased cellularity with minimal nuclear atypia (B). These fragments are adjacent to more classic areas of fibrous dysplasia which exhibit a storiform architecture and trabecular islands of woven bone (C). Higher power examination shows these fragments lack a prominent associated osteoblastic cell population (D).

References:

1. Dahlin DC, Bertoni F, Beabout JW, et al. Fibrocartilaginous mesenchymoma with low-grade malignancy. *Skeletal Radiol.* 1984;12:263-269.
2. Ishida T, Dorfman HD. Massive chondroid differentiation in fibrous dysplasia of bone (fibrocartilaginous dysplasia). *The American journal of surgical pathology.* 1993;17:924-930.
3. Czerniak B, Dorfman HD. *Dorfman and Czerniak's bone tumors*. 2016.

AMR Seminar #77

Case – 8

Contributed by: Fredrik Petersson, M.D.

Clinical History and Gross Features: The patient is a 70 year old Female with a previous history of breast cancer (2016; mixed invasive lobular and tubular), N0 with no recurrence, H.pylori gastritis and type 2 DM.

In 2018 a right renal tumor was picked up on a CT-scan of the abdomen. The tumor was located in the mid to lower pole, with para-pelvic location and measured 4.9 cm. A right nephrectomy was performed and revealed a well demarcated 5.5 x 3.8 x 3.5 cm large tumour, confined to the kidney, with friable cut surface. Subsequently unremarkable gastro- and colonoscopies were performed. Also, a PET CT Gallium-scan was done (negative). The patient is well at 2 years follow-up.

Histological and Immunohistochemical Findings: You have received either one slide exclusively containing neoplastic tissue or one which contains both tumor and renal tissue. In the latter case, the tumor is seen to be well demarcated from the sinus-fat and renal parenchyma. The tumor is composed of anastomosting trabeculae/cords/ribbons with formation of rosette-/duct-like structures and scattered small solid aggregates (mainly on the slide with only tumor tissue). The tumour cells exhibit a range of appearances, from very small dark cells with minimal cytoplasm and small round nuclei, to cells with more abundant eosinophilic cytoplasm and slightly larger ovoid nuclei. The chromatin is fine and stippled and nucleoli are absent to inconspicuous/small. Mitotic activity is low (<1/10hpf). No tumor necrosis was identified. The stroma is vascular.

On immunohistochemistry, the tumor cells show diffuse cytoplasmic expression of synaptophysin with "polar" accentuation, and cytoplasmic expression of chromogranin A and EMA. There is no expression of CK7, AMACR, ER, PR and WT1. On immunohistochemistry, Ki67 expression is low, albeit somewhat variable, on average <3%.

Diagnosis: This is a histologically straight forward case – ***Primary renal neuroendocrine tumor grade 1/carcinoid*** . The location, however, is very uncommon and that is why I wanted to share this case with the members.

Comments: Genitourinary carcinoid tumors (CTs) are uncommon and make up <1% of all CTs and are most commonly seen in the gonads, but may also be encountered in the bladder, prostate and kidney. Since the first description of primary renal CT (Resnick et al, 1966), around 100 cases have been published. Renal CT shows no gender or side predilection. The rarity of CTs in the kidney is related to the fact that neuroendocrine cells are not typically found in the renal parenchyma. The histogenesis is thus unclear. However, neuroendocrine cells are present in the kidney during embryogenesis, and the possibility of having trapped bona fide neuroendocrine cells, or pluripotent stem cells gives a plausible histogenetic explanation. Renal CT is associated with horseshow kidneys and renal teratomas and some data indicate that renal CTs in horsehoe kidneys (often arising from the isthmic part), have different – more benign clinical behavior. Generally, the risk of renal CTs giving rise to metastasis (mainly regional/para-aortic lymph nodes and liver – less common lung, bone, spleen), is related to size (<4 cm low risk) and proliferative activity (Ki-67 >3%, >2-3 mitotic figures/10 HPF). Carcinoid tumors typically grow slowly and are often clinically asymptomatic and picked up as incidental findings on imaging studies for other reasons. Seventy-five percent of primary renal carcinoid tumors are greater than 4 cm and 45% of tumors invade the perirenal or sinus/hilar fat or invade the renal vein. Renal CT may be associated with the paraneoplastic carcinoid-, Cushing- and Verner Morrison- syndromes.

There is nothing "specific" about the histopathologic features or immunohistochemical properties of renal CTs and given the rarity, the diagnosis is thus one of exclusion. The differential diagnosis, especially on a core biopsy, mainly includes:

Metanephric adenoma: Papillary structures in 50% cases – short blunt papillae reminiscent of immature glomeruli. IHC: WT1 +, CD57 +, CK7 – or very focally +. Negative for AMACR, EMA.

Type-1 papillary carcinoma: A range of histopathologic patterns, including solid and tubular architecture. IHC positive for EMA, AMACR, RCC, CD10 and CK7.

PNET: Solid sheets of primitive small uniform cells. IHC CD99, FLI-1, ERG, PAX7, NKX2.2.

Scintigraphy with radiolabelled octreotide or Gallium is useful for detection of occult tumor foci, monitoring metastasis and post-treatment recurrence. Treatment options for renal CTs are partial nephrectomy or cryoablation depending on location and tumor size and radical nephrectomy when the tumor is large. Regional lymph node dissection is typically performed if there is any evidence of enlarged nodes on imaging.

In 2019, Ondrej's group published a paper in Histopathology on NGS findings in renal CTs. Based on 9 cases, they found variable mutational profiles and none of the studied genes/pathways were deemed specific.

Figures:

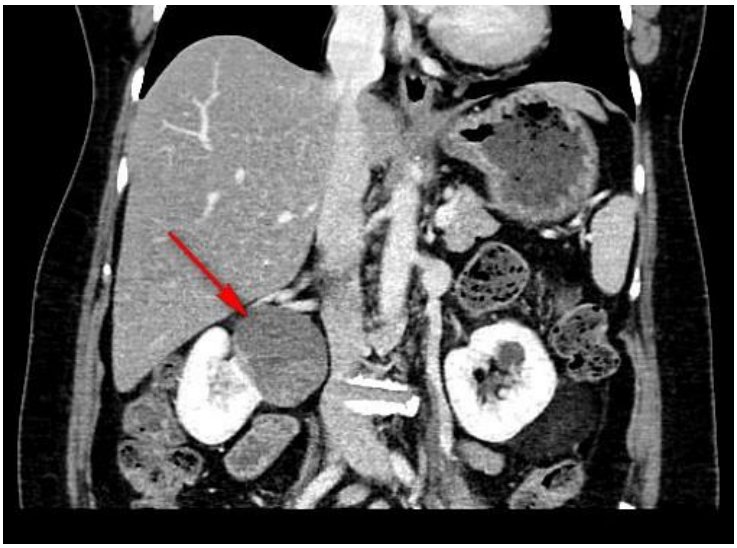

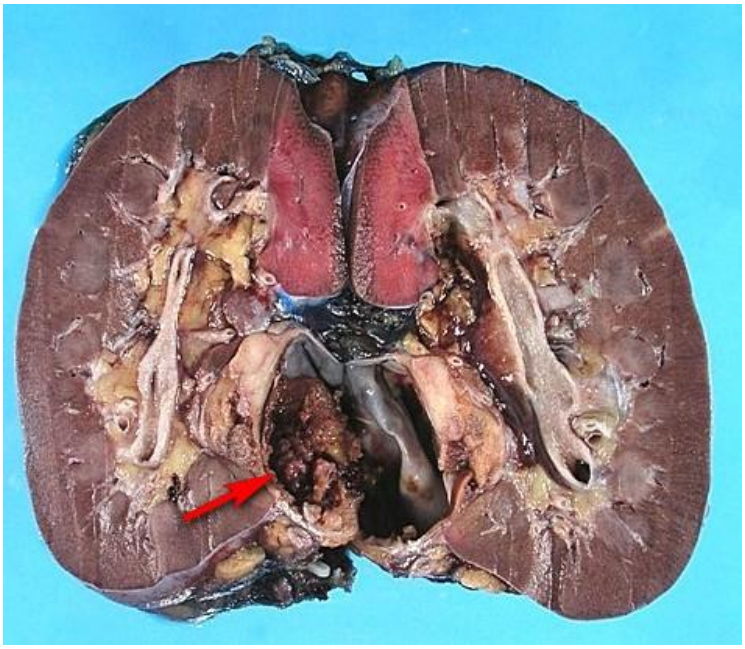

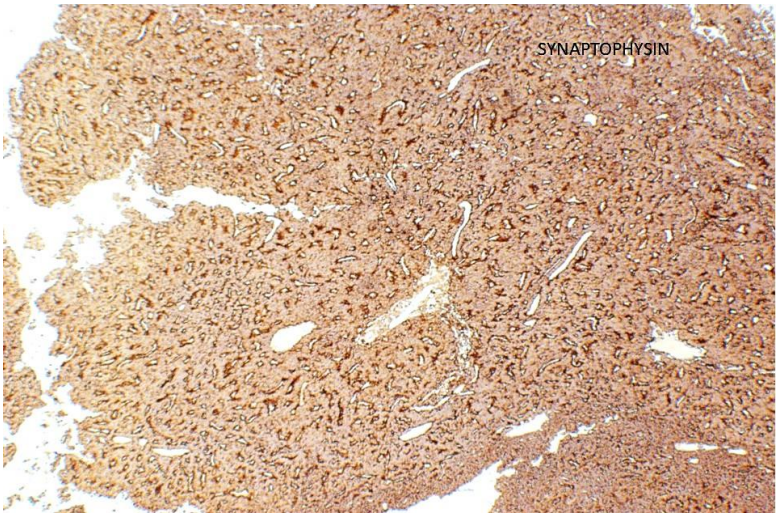
SYNAPTOPHYSIN

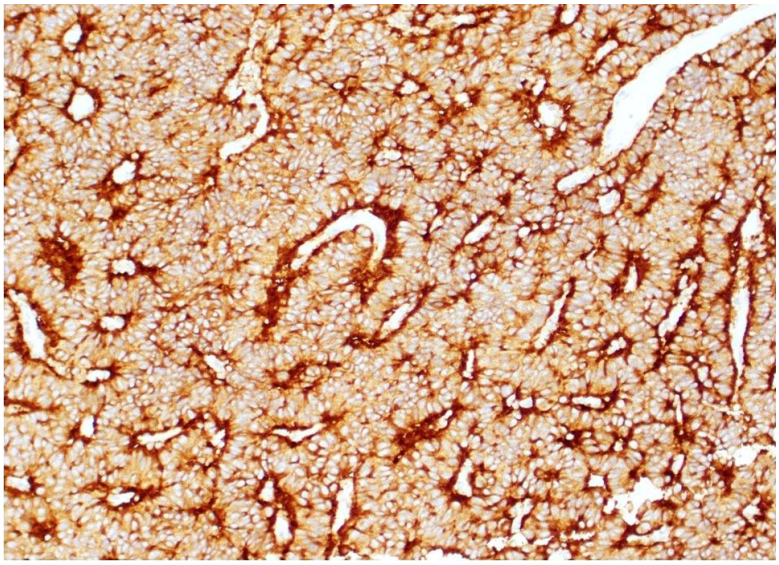

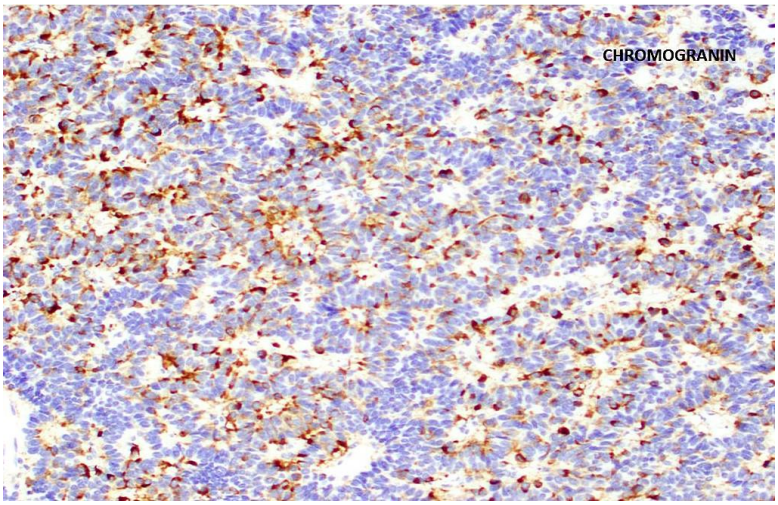

<u>References</u>:

Ayodeji O. Omiyale and Anthony Kodzo-Grey Venyo. Advances in Urology; Volume 2013, Article ID 579396.
Kristyna Varcicova et al. Histopathology 2019, 75: 104-117.

Joel E Rosenberg et al. Pathology & Oncology Research 2020, 26: 341-346.

Bohyun Kim et al. Diagnostic Pathology 2019, 14: 12

AMR Seminar #77

Case – 9

Contributed by: Shira Ronen, M.D.

Clinical History: A 26-day old baby boy is seen for recent growth of a small nodule within a large, map-like congenital nevus extending along the back into the gluteal region for about 20 cm. Areas of the nevus contained hair, others showed variegation in color ranging from pink to dark brown.

Histological and Immunohistochemical Findings: Sections through the specimen shows the characteristic features of congenital giant nevus of the newborn, with densely packed sheets of small round to oval melanocytic cells with hyperchromatic nuclei but devoid of nucleoli admixed with scattered melanin depositions in the stroma. The cellular proliferation penetrated deep into the dermis and infiltrated subcutaneous fat but became more sparsely cellular and progressively collagenized in the deeper portions of the lesion. The small spindle melanocytic cells splayed the collagen in the characteristic fashion of congenital nevi. Located toward one end of the sample was a well-circumscribed, expansile dermal nodule containing slightly larger, epithelioid melanocytes with enlarged vesicular nuclei, prominent nucleoli and very rare mitotic figures. The melanocytes in both components of the lesion were positive for S100 and Melan-A, and a Ki-67 stain showed a mild increase in proliferative activity within the enlarging nodule (~1-2% nuclear positivity) compared with the surrounding melanocytes.

Diagnosis: Proliferative nodule arising in congenital giant nevus.

Comments: Giant congenital melanocytic nevi are defined as a melanocytic lesion that is present at birth and reaches a size >20 cm. The risk for developing a malignant melanoma from a giant congenital nevus has been estimated at 2-6% in the smaller lesions, and up to 20% for giant nevi. In fact, congenital giant nevi are regarded as the main risk factor for the development of malignant melanoma in children. The majority of melanomas arising in congenital giant nevi are of conventional type, although some authors believe that melanomas arising in congenital giant nevus originate from dermal melanocytes rather than from the epidermis. Simulants of nodular melanoma with black nodules composed of epithelioid melanocytes have also been described in these nevi. These have been regarded as proliferative nodules without competence for metastases or invasive growth. Distinction of these nodules from true nodular malignant melanoma is based on degree of cytologic atypia, mitotic activity and elevated Ki-67 proliferation index (>20% nuclear positivity). The differential diagnosis includes a "minimal deviation melanoma", a concept espoused by Richard Reed for low grade melanocytic lesions that is felt to have a less aggressive behavior than other melanoma counterparts, stage for stage. Minimal deviation melanoma is characterized histologically by the expansile growth of uniformly atypical nevomelanocytes in the dermis with extension into the reticular dermis. The concept blends imperceptibly with other borderline melanocytic lesions such as atypical Spitz nevus or Spitzoid melanoma and has been challenged in then literature. This patient is alive and well after 40 years and never experienced progression of the disease or the development of a true metastasizing malignant melanoma. Recognition of the indolent nature of the melanocytic proliferation can be difficult at times but in newborns and young adults, greater tolerance for minimal deviations in melanocytic growths need to be adopted to avoid unnecessary harmful treatment.

References:

1. Belysheva TS et al. Melanoma arising in a giant congenital melanocytic nevus: two case reports. Diagnostic Pathology 2019; 14:21.

2. Watt AJ et al. Risk of melanoma arising in large congenital melanocytic nevi: a systematic review. Plast Reconstr Surg 2004; 113:1968.
3. Phillips ME at al. The spectrum of minimal deviation melanoma: a clinicopathologic study of 21 cases. Hum Pathol 1986; 17:796-806.
4. Reed RJ. Minimal deviation melanoma. Hum Pathol 1990; 21:1206-1211.

AMR Seminar #77

Case – 10

Contributed by: David Suster, M.D.

Clinical History: A 22-year-old man was seen for pain in his right hip. X-rays showed a large lytic mass with loculations and a thin shell of reactive bone surrounding the lesion in the metaphysis of the right femur. The differential diagnosis included aneurysmal bone cyst and fibrous dysplasia. A segmental resection of the proximal end of the femur was performed.

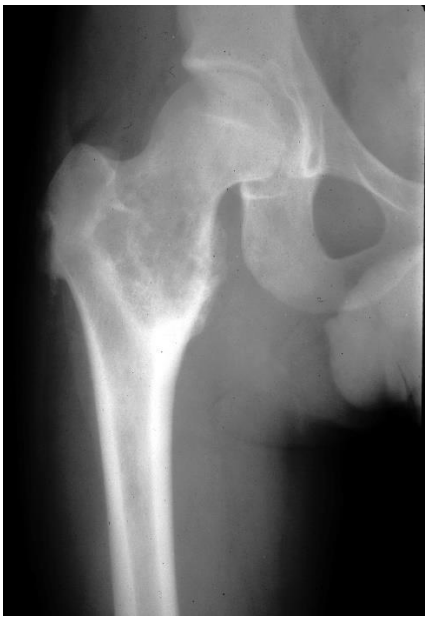

Histological and Immunohistochemical Findings: Review of the histologic sections showed a proliferation of immature woven bone admixed with occasional islands of mature lamellar bone rimmed by numerous large, plump osteoblastic cells. The osteoblastic cells were at least twice the size of conventional osteoblasts. The bony trabeculae were irregular and haphazardly distributed against a fibrovascular stroma with variably sized and dilated blood vessels. The stroma also contained extravasated red blood cells and occasional scattered fibroblastic spindle cells. In the majority of cases, the osteoblastic proliferation formed sheets or clusters of large epithelioid cells in the intertrabecular spaces that were variably admixed with multinucleated osteoclastic giant cells. The epithelioid mononuclear cells displayed large round to oval nuclei with prominent nucleoli and were surrounded by an ample rim of basophilic to eosinophilic cytoplasm. Occasional large, atypical cells with bizarre, densely hyperchromatic nuclei, could also be seen. Rare mitotic figures were identified, but abnormal mitoses were not seen. The tumor showed ABC-like changes with abundant hemorrhage and hemosiderin deposition. Immunostains showed nuclear positivity for FOS antibodies.

Diagnosis: Epithelioid osteoblastoma.

Comments: Osteoblastoma is a rare bone tumor that most often affects the spine of individuals between 10-30 years of age but may affect virtually any bone. The tumor is characterized by an exuberant production of bone

spicules rimmed by abundant osteoclasts and separated by a fibrovascular stroma containing scattered osteoclastic giant cells. The lesions are histologically indistinguishable in many cases from osteoid osteoma, except they are much larger (>1 cm, in diameter). Osteoblastoma is known to exhibit a spectrum of histologic features that can be quite variable, including the occasional presence of histologic and radiologic atypical features. The terms "atypical osteoblastoma" and "aggressive osteoblastoma" have been used interchangeably in the past for tumors that showed either atypical histologic features or displayed unusually aggressive and locally destructive behavior with local recurrences. The term "epithelioid osteoblastoma" has also been used to designate tumors in which clusters of large osteoblasts with a striking epithelioid morphology are seen. The term currently favored by the WHO for these tumors, however, is epithelioid osteoblastoma.

In recent years, FOS and FOSB overexpression has been demonstrated in osteoblastomas. It was postulated that this could be a valuable adjunct to diagnosis in equivocal cases. We attempted to do FISH in our lab for FOS and FOSB in 12 of our cases but were unable to obtain any results. Dr. Mackinnon also attempted to do NGS on these tumors in his lab but was unable to obtain quality DNA for the assay, most likely due to the decalcification status of the cases. We also performed immunohistochemical staining for both FOS and FOSB with inconsistent results. H&E still remains the most reliable tool for diagnosis, coupled with the clinical and radiological findings.

With the increasing use of CT-guided core needle biopsies for the preoperative evaluation of bone tumors, the potential for overdiagnosis of the epithelioid variant of osteoblastoma has become apparent. We recently studied 19 examples of osteoblastoma (of which this is one of the cases) that were characterized by a predominantly epithelioid morphology. In three of our patients, core needle biopsies were interpreted as suspicious or consistent with osteosarcoma due to the striking cytologic atypia displayed by the tumor cells; in one of the patients the core needle biopsy diagnosis led to neoadjuvant chemotherapy and a distal femur resection, with the true nature of the lesion only becoming appreciated on the resection specimen. Radiological correlation is essential for the interpretation of bone tumors; however, it should be noted that the radiologic diagnosis of osteoblastoma is not always straightforward, and the radiologist may not always be able to offer a definitive diagnosis. In our study, the imaging studies were felt to be consistent with osteoblastoma in only 6/11 cases. However, information regarding whether the radiologist has found evidence of an aggressive or malignant neoplasm will always be helpful in this context to avoid missing a diagnosis of malignancy.

Although epithelioid morphology has often been associated with a more aggressive behavior in osteoblastoma, the results of our study appear to indicate that this is not necessarily always the case, and epithelioid morphology can also be seen in cases that are small, well-circumscribed and non-invasive that follow a benign course. The term epithelioid osteoblastoma is preferrable in this setting to that of aggressive osteoblastoma to highlight the atypical morphology but without the suggestion of aggressive behavior. The main importance of recognizing this morphologic variant of osteoblastoma lies in avoiding a misdiagnosis of malignancy that could result in unnecessarily aggressive treatment.

References:

1. Lucas DR, Unni KK, McLeod RA, O'Connor MI, Sim FH. Osteoblastoma: Clinicopathologic study of 306 cases. Hum Pathol 1994; 23:117-134.
2. Dorfman HD, Weiss SW. Borderline osteoblastic tumors: problems in differential diagnosis of aggressive osteoblastoma and low-grade osteosarcoma. Semin Diagn Pathol 1984;1:215-234.
3. Lucas DR. Osteoblastoma. Arch Pathol Lab Med 2010;134:1460-1466.
4. Fittal MW, Mifsud W, Pillay N, Ye H, Strobi A-C, Verfaillie A et al. Recurrent rearrangements of *FOS* and *FOSB* define osteoblastoma. Nature 2018;9:2150.
5. Suster D, Mckinnon AC, Jarzembowski J, Carrera G, Klein MN. Epithelioid osteoblastoma: Clinicopathologic and immunohistochemical study of 19 cases (submitted)

AMR Seminar #77

Case – 11

Contributed by: Ady Yosepovich, M.D.

Clinical History: This is a nice 50-year-old patient who underwent lumpectomy due to left breast 6 mm area of micro-calcifications that were inspected in routine mammogram.

Breast US was negative; breast MRI showed 15 mm density in the same area.

Vacuum assisted XR guided CNB showed high-grade comedo-type apocrine DCIS.

Lumpectomy and SLN biopsy were performed. The lumpectomy specimen showed an irregular 1.5 cm mass. The lymph nodes were free of tumor. The slide submitted represents the mass.

Microscopic Features: A tumor composed of atypical cells and glandular structures with pink cytoplasm, large nuclei with distinctive nucleoli. Apocrine DCIS is also present.

Histological and Immunohistochemical Findings: Pan Keratin and E-cadherin stains are positive in the tumor cells. ER, PR, HER-2 are all negative. Ki-67 shows low proliferative activity (10%).

Diagnosis: Invasive Apocrine Carcinoma.

Comments: I send you this case because it is not the first time I noticed that triple negative apocrine carcinomas can have low proliferative index. It is known in the literature that there are special triple negative breast carcinoma subtypes with favorable prognosis. Apocrine carcinomas are not included in this list. I would very much like to know if you have some experience or thoughts concerning this subject – as a rule those patients get chemotherapy (1.5 cm triple negative carcinoma) – I doubt if it is necessary in this particular case with low mitotic activity tumor.

AMR SEMINAR #77

CASE #12

Contributed by: Saul Suster, M.D.

Clinical History: A 52-year-old man with a history of diabetes insipidus was seen 6 years ago for superficial soft tissue mass on his right posterior shoulder region. The mass measured 3.0 x 3.0 x 2.8 cm. and was painless, moveable, and subcutaneous, and had been present for several years. The mass was excised (the current sample) and was diagnosed as a "benign fibrohistiocytic tumor with abundant xanthoma cells". The histiocytic cells were strongly positive for CD163 and CD68, and negative for S100 and CD31. PAS stain was negative and Fite-Faraco stain did not reveal any organisms. Two years later, a well-circumscribed soft tissue nodule was removed from the left orbital region, measuring 2.0 x 2.0 x 1.5 cm. It was signed out as "diffuse xanthogranulomatous inflammation". More recently the patient was evaluated for pain and weakness in his knees, and X-rays and MRI disclosed osteosclerosis of his distal femur. A core biopsy showed features consistent with Erdheim-Chester disease. BRAF V600e study is pending.

Diagnosis: Xanthogranulomatous process consistent with Erdheim-Chester disease.

Comment: We have seen cases of Erdheim-Chester disease in the pleura and lungs previously, and also in bone. I have also seen a few rare cases of involvement in other organs, including heart and omentum, but I had never seen one involving soft tissue or presenting as a soft tissue mass. Has anyone had experience with subcutaneous or soft tissue involvement with Erdheim-Chester disease? This was a new one for me.

AMR SEMINAR #77

Quiz Case 1

Contributed by: Saul Suster, M.D.

Clinical History: An 81-year-old woman with no previous significant history was seen for shortness of breath and cough. Imaging studies revealed an irregular 2.1 cm. mass in her right upper lobe of lung. A surgical resection of the lesion was performed which revealed an intermediate grade neuroendocrine carcinoma (atypical carcinoid) that was stage T1b, N0, MX. At the time of surgery, the surgeon noted a 2 cm. indurated nodule in the parietal pleura at the level of the right lower lobe suspicious for a metastasis. Histologic examination of this nodule shows dense thickening of the pleura with fibrosis and an apparently-bland, sparse spindle cell proliferation in the stroma. The lesion was ill-defined and not well circumscribed and appeared to be infiltrating the pleural fat. Immunohistochemical stains showed the tumor cells were negative for cytokeratin AE1/AE3 and CAM5.2, CK5/6, calretinin, HBME1, pCEA, TTF1, SMA, desmin, CD34, S100 protein and WT1. The only positive stain was vimentin.